Journal of Inorganic Biochemistry xxx (2015) xxx–xxx

Contents lists available at ScienceDirect

Journal of Inorganic Biochemistry

journal homepage: www.elsevier.com/locate/jinorgbio

Insights into the strong in-vitro anticancer effects for bis(triphenylphosphane)iminium compounds having perchlorate, tetrafluoridoborate and bis(chlorido)argentate anions

Alessandra Folda [a,1], Valeria Scalcon [b,1], Mohamed Ghazzali [c], Mohammed H. Jaafar [c], Rais Ahmad Khan [c], Angela Casini [d], Anna Citta [a], Alberto Bindoli [b], Maria Pia Rigobello [a,*], Khalid Al-Farhan [c], Ali Alsalme [c], Jan Reedijk [c,e,**]

[a] Department of Biomedical Sciences, University of Padova, via Ugo Bassi 58/b, 35131 Padova, Italy
[b] Institute of Neuroscience (CNR), viale G. Colombo 3, 35131 Padova, Italy
[c] Department of Chemistry, College of Science, King Saud University, P.O. Box 2455, Riyadh 11451, Kingdom of Saudi Arabia
[d] Department of Pharmacokinetics, Toxicology and Targeting, Groningen Research Institute of Pharmacy, University of Groningen, Antonius Deusinglaan 1, 9713 AV Groningen, The Netherlands
[e] Leiden Institute of Chemistry, Leiden University, P.O. Box 9502, 2300 RA Leiden, The Netherlands

ARTICLE INFO

Article history:
Received 26 July 2015
Accepted 28 August 2015
Available online xxxx

Keywords:
Isomorphism
Anti-cancer compounds
Crystal structure
DNA binding
Mitochondria
Thioredoxin reductase

ABSTRACT

Three new compounds containing the bis(triphenylphosphane)iminium cation (PPN^+) with ClO_4^-, BF_4^- and $[AgCl_2]^-$ as counter anions have been synthesized and structurally characterized. The two derivatives with ClO_4^- and BF_4^- were found to be isostructural by single crystal X-ray diffraction. Interestingly, the three compounds show extremely potent antiproliferative effects against the human cancer cell line SKOV3. To gain insights into the possible mechanisms of biological action, several intracellular targets have been considered. Thus, DNA binding has been evaluated, as well as the effects of the compounds on the mitochondrial function. Furthermore, the compounds have been tested as possible inhibitors of the seleno-enzyme thioredoxin reductase.

1. Introduction

The bis(triphenylphosphane)iminium cation (often abbreviated as PPN^+) is a classical cation, known to be useful in the isolation of reactive anions. The distinguished ability of PPN^+ in stabilizing air-sensitive, less-stable metallic anions is the reason for its popularity in the synthesis of many unique organometallic and coordination compounds. For example, it is known that many important and unique chemo-physical phenomena can arise when trapping an interesting anion in a chemically inert solid phase. Thus, the first known crystal structures of fullerene C_{60} were only achievable using the PPN^+ as the counter ion [1,2], while the compound PPN^+-(bipyridyl)tetracyanidoruthenate is a technologically efficient humidity sensor [3].

Another reason of the growing uses of PPN^+ arose after its degree of bent vs. linear geometrical flexibility had been disclosed [4]. In fact, it is unsurprising that 1453 crystal structures incorporating PPN^+ are counted in the Cambridge Structural Database [5], of which a majority of ca. 90% is incorporating anionic metal complexes. The rest of reported PPN^+ compounds with simple metallic-free anions is also of remarkable importance. For example, the bis(triphenylphosphane)iminium nitrite is reported as a versatile nitrosylating reagent [6], and the bis(triphenylphosphane)iminium nitrate is a known nitrate-sensitive electrode [7].

Unfortunately, structurally-reported compounds of PPN^+ containing small anions are scarce, namely those with thiocyanate [8], monothionitrate [9], perthionitrite [10], iodate [11], tri-iodide [12] and chloride [13] anions. Also, the crystal structure of PPN^+ with tetrafluoridoborate mono(dichloromethane) is known [14]. None of these compounds has ever been characterized for its biological properties and its effects on cancer cell lines. We hypothesized that PPN^+ may behave as a so-called membrane permeable Delocalized Lipophilic Cation (DLC) which can target mitochondria and exert cytotoxic effects [15].

Mitochondria are known to play a major role in cell energy metabolism as they generate ATP (adenosine triphosphate) following oxidation of respiratory substrates. Furthermore, they are also involved in the modulation of Ca^{2+} homeostasis, in ROS (Reactive Oxygen Species) production and in stimulation of the intrinsic pathway to cell apoptosis.

* Correspondence to: M. P. Rigobello, Dipartimento di Scienze Biomediche, University of Padova, via Ugo Bassi 58/b, 35131 Padova, Italy.
** Correspondence to: J. Reedijk, Leiden Institute of Chemistry, Leiden University, P.O. Box 9502, 2300 RA Leiden, The Netherlands.
E-mail addresses: mariapia.rigobello@unipd.it (M.P. Rigobello), reedijk@chem.leidenuniv.nl (J. Reedijk).
[1] These two authors contributed equally to this paper.

http://dx.doi.org/10.1016/j.jinorgbio.2015.08.030

Mitochondria, once energy generated by the oxidation of substrates is stored as electrochemical potential, develop a membrane potential of about 180 mV, that is used for ATP formation and ion transport. As this membrane potential is negative inside, the molecules endowed with a positive charge distributed over a broad surface area such as DLC, can be accumulated in the mitochondrion. These molecules are first driven into the cell by the plasma membrane potential and then, from the cytosol, they can concentrate in the mitochondrial matrix [16].

Several cancer cell lines present a higher plasma and mitochondrial membrane potential in comparison to normal cells; this condition has been exploited for targeting lipophilic cations with potential anticancer action to mitochondria [17–20]. In the mitochondrial matrix, the thioredoxin system represents a major pathway involved in the removal of dihydrogen peroxide and in thiol-dependent redox regulation. The thioredoxin system is composed of NADPH, thioredoxin reductase and thioredoxin. NADPH, through thioredoxin reductase, maintains thioredoxin reduced, in turn able to act as a substrate of peroxiredoxin that very efficiently removes dihydrogen peroxide. Thioredoxin reductase is reported to be inhibited by a large number of molecules most of which are anticancer agents [21].

Within this frame, we are reporting here the synthesis, characterization, crystal structures, anti-proliferative and DNA-binding studies, the effects on mitochondria functions and mitochondrial thioredoxin reductase activity of bis(triphenylphosphane)iminium perchlorate, onwards denoted as **1**, bis(triphenylphosphane)iminium tetrafluoridoborate, onwards denoted as **2** and of bis(triphenylphosphane)iminium [dichloridoargentate(I)] monoethanol, onwards denoted as **3**, see Fig. 1 for the schematic structures.

2. Experimental

2.1. Materials and methods

Melting points were determined on an electrothermal's IA9000 series digital capillary melting point apparatus and are uncorrected. FT-IR spectra were measured using a KBr pressed disk on a Shimadzu IR-Affinity spectrophotometer (4000–400 cm^{-1}). X-ray powder diffraction was carried out for the sake of confirming phase purity, using Rigaku Ultima-IV equipment with copper radiation and Bragg–Brentano geometry. The elemental analyses were performed by using a Perkin Elmer Series II-2400 analyzer.

The starting chemicals, $[N(PPh_3)_2]^+Cl$, KCN, Ag(CN) and Au(CN) and solvents were used as commercially available (BDH-Analar grade). Hexane and acetone were kept over molecular sieves. The compounds $[N(PPh_3)_2][Ag(CN)_2]$ and $[N(PPh_3)_2][Au(CN)_2]$ were prepared as described below.

2.2. Synthesis

Synthesis of $[N(PPh_3)_2][Au(CN)_2]$: gold cyanide $[Au(CN)]_n$ (0.223 g, 1 mmol) was added to a solution of KCN (0.065 g, 1 mmol) in methanol (20 mL). After a clear solution had been obtained, $[N(PPh_3)_2]^+Cl^-$ (0.574 g, 1 mmol) was added to the reaction mixture. Stirring was continued for 15 min. The solution was evaporated to dryness and the white residue was treated with acetone (25 mL). The remaining solid, KCl (0.050 g), was filtered off. Addition of hexane to the filtrate resulted in white crystals of $[N(PPh_3)_2][Au(CN)_2]$ (0.750 g, 95%), m.p. 209 °C. Elemental analysis: found: C, 57.64; H, 4.19; N, 4.12. Calc. for: $C_{38}H_{30}AuN_3P_2$: C, 57.94; H, 3.81; and N, 5.3.

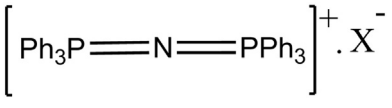

Fig. 1. Schematic representation of $[PPN]^+X^-$ compounds; in reality the P-N-P angle is often bent by some 140°.

Synthesis of $[N(PPh_3)_2][Ag(CN)_2]$. Silver cyanide $[Ag(CN)]_n$ (0.134 g, 1 mmol) was added to a solution of KCN (0.065 g, 1 mmol) in methanol (40 mL). After a clear solution had been obtained, $[N(PPh_3)_2]^+Cl^-$ (0.574 g, 1 mmol) was added to the reaction mixture. Stirring was continued for 15 min. The solution was evaporated to dryness and the white residue was treated with acetone (30 mL). The remaining solid, KCl (0.065 g), was filtered off. Addition of hexane to the filtrate resulted in white crystals of $[N(PPh_3)_2][Ag(CN)_2]$ (0.663 g, 95%), m.p. 90 °C. Elemental analysis: found: C, 65.99; H, 4.55; N, 5.18. Calc. for: $C_{38}H_{30}AgN_3P_2$, C, 65.33; H, 4.30; and N, 6.01.

Compound **1**: silver perchlorate $AgClO_4$ (0.208 g, 1 mmol) was added to a clear solution of $[N(PPh_3)_2][Ag(CN)_2]$ (0.698 g, 1 mmol) in acetone (20 mL). Immediately, a white precipitate was formed. Stirring was continued for 90 min at room temperature, the precipitate was filtered off, washed with acetone (10 mL), and collected as Ag(CN) (0.260 g, 97%), m.p. decomposition at 300 °C. Addition of hexane (30 mL) to the filtrate resulted in white crystals of $[N(PPh_3)_2]ClO_4$ (0.5 g, 94%), m.p. 265 °C. Elemental analysis: found: C, 67.70; H, 4.29; N, 1.96. Calc. for $C_{36}H_{30}NClO_4P_2$: C, 67.87; H, 4.71; and N, 2.19%. The IR spectrum was found to be typical for the PPN cation and a strong peak assigned to perchlorate (near 1090 cm^1).

Compound **2**: silver tetrafluoridoborate $AgBF_4$ (0.195 g, 1 mmol) was added to a clear solution of $[N(PPh_3)_2][Au(CN)_2]$ (0.787 g, 1 mmol) in acetone (25 mL). Immediately a white precipitate was formed. Stirring was continued for 90 min at room temperature, the solid was filtered off, washed with acetone (10 mL), and identified as $AuAg(CN)_2$ (0.325 g, 91%), m.p. decomposition at 335 °C. Addition of hexane (30 mL) to the filtrate gave white crystals of $[N(PPh_3)_2]BF_4$ (0.590 g, 94.4%), m.p. 240 °C. Elemental analysis: found: C, 69,70; H, 4.75; N, 2.19. Calc. for $C_{36}H_{30}NBF_4P_2$: C, 69.12; H, 4.8; and N, 2.22%. The IR spectrum was found to be typical for the PPN cation and a strong peak assigned to tetrafluoridoborate (near 1050 cm^1).

Compound **3**: silver(I) chloride AgCl, (0.143 g, 1 mmol) was added to a clear solution of bis(triphenylphosphane)iminium chloride, $[N(PPh_3)_2]^+Cl^-$ (0.574 g, 1 mmol), in methanol (35 mL). Stirring continuously under nitrogen gas and heating at 60 °C for 30 min, resulted in a clear solution. Addition of diethyl ether (20 mL) to this clear solution resulted in a crystalline solid, which was filtered off and from which light pale yellow crystals were collected as $[N(PPh_3)_2]^+[ClAgCl]^-\cdot CH_3CH_2OH$, (0.712 g, 95%), dec. at 170 °C and melting at 272 °C. Elemental analysis: found: C, 60.00; H, 4.65; N, 2.19. Calc. for. $C_{36}H_{36}AgNCl_2OP_2$: C, 59.76; H, 4.72; N, 1.83%. The IR spectrum was found to be typical for the PPN cation. Bands due to $[ClAgCl]^-$ were not found above 400 cm^1.

2.3. X-ray crystallography

Suitable colorless plate crystals of the compounds **1**, **2** and **3** were selected under an optical microscope, glued and mounted onto a thin glass capillary. Diffraction data were collected for **1** and **2** at 294 K, and for **3** at 173 K using Rigaku *R*-axis diffractometer equipped with an imaging plate detector, utilizing graphite-monochromatised Cu-K_α in **1–2** and Mo-K_α radiations in **3**. Full spheres of reciprocal spaces were using the ω-scan. Preliminary orientation matrices, unit cell determination and data reduction and corrections were performed using the *CrystalClear* package [22]. The structures were solved by direct methods and refined by full-matrix least squares on all $|F^2|$ data, using the *SHELX* package [23]. Hydrogen atoms were isotropically refined and constrained to ideal geometry, using their appropriate riding model and all non-hydrogen atoms were anisotropically refined. The perchlorates and tetrafluoridoborates in **1** and **2** were constrained to ideal geometry, using appropriate geometrical restraints. The relatively high R value (9.8%) for compound **1** is due to poor crystal quality; the isomorphism with compound **2** gives confidence for its accuracy. Fig. 1 was created using the *DIAMOND* package [24]. Crystallographic parameters of

Please cite this article as: A. Folda, et al., Insights into the strong in-vitro anticancer effects for bis(triphenylphosphane)iminium compounds having perchlorate, tetrafluorid..., J. Inorg. Biochem. (2015), http://dx.doi.org/10.1016/j.jinorgbio.2015.08.030

compounds **1**–**3** are summarized in Table 1, while selected geometrical parameters are discussed and presented below.

2.4. Antiproliferative assays

The human ovarian cancer SKOV3 cells, (obtained from the European Centre of Cell Cultures ECACC, Salisbury, UK) were cultured in DMEM containing GlutaMAX-I supplemented with 10% FBS and 1% penicillin/streptomycin (all from Invitrogen), at 37 °C in a humidified atmosphere of 95% of air and 5% CO_2 (Heraeus, Germany). For evaluation of growth inhibition, cells were seeded in 96-well plates (Costar, Integra Biosciences, Cambridge, MA) at a concentration of 10,000 cells/well and grown for 24 h in complete medium. Solutions of the compounds were prepared by H_2O and appropriate dilutions in DMEM were added to the wells (200 μL) to obtain a final concentration ranging from 0.01 to 50 μM. Following 72 h drug exposure, 3-(4,5-dimethylthiazol-2-yl)-2,5-diphenyltetrazolium bromide (MTT) was added to the cells at a final concentration of 0.50 $mg \cdot mL^{-1}$ and incubated for 3–4 h, time after which the culture medium was removed and the violet formazan crystals dissolved in DMSO. The optical density of each well (96-well plates) was quantified in quadruplicate at 540 nm, using a multi-well plate reader, and the percentage of surviving cells was calculated from the ratio of absorbance between treated and untreated cells. The IC_{50} value was calculated as the concentration reducing the proliferation of the cells by 50% and is presented as an average (±SD) of at least three independent experiments.

2.5. DNA binding

The interaction of the compounds (**1**–**3**) with CT-DNA was carried out in buffer containing 5 mM tris(hydroxymethyl)aminomethane buffer adjusted to pH 7.2 with 1 M hydrochloric acid. The CT-DNA dissolved in this Tris–HCl buffer was dialyzed against the same buffer overnight. Solutions of CT-DNA gave ratios of UV absorbance at 260 and 280 nm above 1:1.9, indicating suitable DNA (free of protein). Absorption spectroscopy was used to determine the DNA concentration, using the molar absorption coefficient 6600 $dm^3 \cdot mol^{-1} cm^{-1}$ per nucleotide at 260 nm. The stock solution was kept at 4 °C. The Shimadzu UV-2450 UV–Vis spectrophotometer was used to record absorption and the ethidium bromide displacement assay using a JASCO F 6500 spectrofluorophotometer. The DNA-binding experiments include absorption spectral studies and fluorescence conform to standard methods [25–27] and have been reported earlier [28–30]. Absorption spectral titration experiments were performed by upholding a constant concentration of the complexes and varying the calf thymus DNA (CT DNA) concentration by dissolving an appropriate amount of the compound and DNA stock solutions, while maintaining the total volume constant (3 mL). The ethidium bromide displacement assay was carried out by fixing the excitation wavelength. The DNA was pretreated with ethidium bromide, [DNA/EthBr] = 10 for 30 min at 25 °C. Then the compounds were added to this mixture and their effect on the emission intensity was measured.

2.6. Mitochondrial functions

2.6.1. Preparation of rat liver mitochondria

Mitochondria were prepared from rat liver by differential centrifugations following the procedure of Myers and Slater [31] in a medium containing 220 mM mannitol, 70 mM sucrose, 0.1 mM H_4edta and 5 mM Hepes/Tris buffer (pH 7.0). H_4edta was omitted in the final washing and in the mitochondrial suspension. Mitochondrial proteins were estimated with the biuret procedure [32].

2.6.2. Estimation of mitochondrial swelling

Mitochondrial swelling was followed spectrophotometrically as a decrease of the optical density at 540 nm. Briefly, rat liver mitochondria (0.25 mg/mL) were incubated at 25 °C in 213 mM mannitol, 71 mM sucrose, 5 mM Hepes/Tris buffer (pH 7.4), 5 mM succinate, 5 μM rotenone and 2.5 μM oligomycin in the presence of compounds **1**–**3**.

2.6.3. Mitochondrial dioxygen consumption

Dioxygen uptake was measured polarographically, utilizing a Clark-type oxygen electrode inserted in a water jacketed chamber (25 °C) with constant stirring. Data were acquired and analyzed as described in [33]. Briefly, rat liver mitochondria (1 mg/mL) were incubated at 25 °C in 0.1 M sucrose, 50 mM KCl, 1 mM $MgCl_2$, 1 mM NaH_2PO_4 and 20 mM Hepes/Tris buffer (pH 7.4) and 1 mM H_4egta. Compounds **1**–**3** were added and, after 1 min, respiration was started by 7.5 mM succinate. The consumption of dioxygen was calculated in nmoles of O_2 $sec^{-1} \cdot mg^{-1}$ of protein.

2.6.4. Determination of membrane potential in isolated mitochondria and in cancer cell

The mitochondrial membrane potential was estimated by means of the fluorescent dye rhodamine 123. Mitochondrial proteins (0.6 mg/mL) were incubated at 25 °C in 100 mM sucrose, 50 mM KCl, 20 mM Hepes/Tris buffer (pH 7.4), 1 mM NaH_2PO_4, 1 mM $MgCl_2$, 12.5 μM rotenone, and 0.5 μM oligomycin. Mitochondria were treated with 5 mM succinate as an oxidizable substrate. After 4 min, complexes **1**–**3** were added. Fluorescence was estimated in a microplate

Table 1
Crystal data and refinement details for compounds **1**–**3**.

Crystallographic parameters	1	2	3
Formula	$C_{36}H_{30}NP_2.ClO_4$	$C_{36}H_{30}NP_2.BF_4$	$C_{36}H_{30}NP_2$, $AgCl_2.C_2H_6O$
Formula weight	638.00	625.36	763.39
Crystal system	Monoclinic	Monoclinic	Monoclinic
Space group	P2/n	P2/n	$P2_1/c$
a [Å]	15.3547(3)	15.3592(3)	9.1448(8)
b [Å]	14.0504(3)	13.9495(3)	23.7695(18)
c [Å]	16.2237(3)	16.2115(3)	17.0796(14)
beta [°]	112.340(1)	112.454(1)	101.480(2)
V [$Å^3$]	3237.40(11)	3210.04(11)	3638.3(5)
Z	4	4	4
D(calc) [g/cm^3]	1.309	1.294	1.394
Radiation [Å]	1.54187	1.54187	0.71075
Theta min-max [°]	6.6–72.3	6.6–72.3	3.1, 27.5
Dataset	−18:18; −17:17; −18:18	−18:18; −16:17; −17:18	−11:11; −30:30; −22:22
Tot., uniq. data, R(int)	33220, 5994, 0.042	41145, 5915, 0.031	53543, 8317, 0.134
Observed data [$I > 2\delta(I)$]	3406	2599	4773
Nref, Npar, restraints	5994, 400, 16	5915, 400, 16	8317, 409, 0
R, wR_2, S	0.098, 0.2483, 1.23	0.075, 0.2233, 1.16	0.0746, 0.2280, 1.04
Min., max. resd. dens.	−1.22, 0.85	−0.70, 0.66	−1.04, 0.97

Please cite this article as: A. Folda, et al., Insights into the strong in-vitro anticancer effects for bis(triphenylphosphane)iminium compounds having perchlorate, tetrafluorid..., J. Inorg. Biochem. (2015), http://dx.doi.org/10.1016/j.jinorgbio.2015.08.030

Table 2
Selected bond distances (Å) and angles (°) for compounds **1**–**3**.

Geometrical parameters	1	2	3
P1–N1	1.577(3)	1.575(3)	1.589(5)
P1–C1	1.800(6)	1.792(6)	1.774(7)
P1–C7	1.756(8)	1.805(6)	1.788(8)
P1–C13	1.785(6)	1.778(7)	1.807(7)
P2–N2	1.573(3)	1.578(3)	.....
P2–N1	.....	.....	1.590(5)
P2–C19	1.808(7)	1.778(6)	1.779(8)
P2–C25	1.772(6)	1.803(6)	1.783(7)
P2–C31	1.774(7)	1.797(6)	1.787(7)
Cl1–O1	1.343(11)	.....	.....
Cl1–O2	1.320(8)	.....	.....
F1–B1	.....	1.258(14)	.....
F2–B1	.....	1.235(10)	.....
Ag1–Cl1	.....	.....	2.563(8)
Ag1–Cl2	.....	.....	2.570(7)
N1–P1–C1	113.0(3)	112.5(3)	107.6(3)
N1–P1–C7	109.9(2)	114.4(3)	112.9(3)
N1–P1–C13	107.3(3)	108.3(3)	113.4(3)
C1–P1–C7	109.6(3)	106.2(3)	108.9(4)
C1–P1–C13	107.1(3)	107.8(3)	105.6(3)
P1–N1–P1^{i}	137.7(5)	141.4(4)	.....
P1–N1–P2	.....	.....	136.2(4)
O1–Cl1–O2	111.5(7)	.....	.....
O1–Cl1–O1	100.7(7)	.....	.....
O1–Cl1–O2^{i}	110.2(6)	.....	.....
O2–Cl1–O1^{i}	110.2(6)	.....	.....
O2–Cl1–O2^{i}	112.2(5)	.....	.....
O1^{i}–Cl1–O2^{i}	111.5(7)	.....	.....
F1–B1–F2	.....	112.2(6)	.....
F1–B1–F1^{iii}	.....	97.4(11)	.....
F1–B1–F2^{iii}	.....	108.8(6)	.....
F2–B1–F1^{iii}	.....	108.8(6)	.....
F2–B1–F2^{iii}	.....	115.9(11)	.....
F1^{iii}–B1–F2^{iii}	.....	112.2(6)	.....
Cl1–Ag1–Cl2	.....	.....	178.8(2)

Symmetry codes: (**1**) i: 1/2-x,y,3/2-z and (**2**) i: 3/2-x,y,1/2-z, and iii: 5/2-x,y,3/2-z.

reader (Tecan Infinite® M200 PRO), in a final volume of 0.250 mL, at 485 nm (excitation wavelength) and 527 nm (emission wavelength).

Membrane potentials of human cisplatin-sensitive ovarian cancer cells A2780 were analyzed using flow cytometry. Cells were grown at 37 °C in a 5% CO_2 using RPMI 1640 medium, supplemented with 50 units·mL^{-1} penicillin and 50 μg·mL^{-1} streptomycin, 2 mM L-glutamine, containing 10% fetal calf serum. The changes of the membrane potential induced by the compounds were estimated with a FACSCanto™ II (Becton Dickinson) cytofluorometer using tetramethylrhodamine (TMRM) as a fluorescent dye, with an argon laser at 585 nm.

2.6.5. Thioredoxin reductase inhibition studies

Cytosolic thioredoxin reductase (TrxR1) was prepared from rat liver according to Luthman and Holmgren [34], and mitochondrial thioredoxin reductase (TrxR2) was purified according to Rigobello and Bindoli [35].

The protein content of isolated enzymes was estimated according to Lowry et al. [36]. Thioredoxin reductase activity was measured at 25 °C in 0.2 M Tris/HCl buffer (pH 8.1), and 0.25 mM NADPH. The reaction was started by the addition of 1 mM DTNB (DNTB = 5,5′-dithiobis-2-nitrobenzoic acid; Ellman's reagent) and followed spectrophotometrically at 412 nm.

3. Results and discussion

3.1. Synthesis and 3D structure of the compounds

The synthesis of the three compounds went rather straightforward, despite the unusual recipe starting from bis(cyanido)metallates(I) for compounds **1** and **2** and yielded pure, crystalline homogeneous materials, from which crystals for X-ray diffractions were easily obtained. Using alternative synthetic methods, by using (PPN)Cl and silver salts, did not yield pure compounds. Compounds **1** and **2** were found to be isostructural with no interactions between the cation and the anion. The crystal data and refinement details for all 3 compounds were mentioned in Table 1 (above). Relevant bond lengths and angles are in Table 2. The molecular structures and packing are given in Fig. 2.

In addition to the intrinsic intramolecular C–H…N hydrogen bonding in the PPN molecular structures, the molecular packing in **1** and **2** are supported with weak C–H…O and C-H…F intermolecular hydrogen bonding. The molecular arrangement in **3** is dominated by weak C–H…Cl hydrogen bonding interactions.

The intramolecular distances for the cation and the anion, are all uneventful. Compound **3** contains an ethanol solvent molecule filling a gap in the crystal lattice; in fact this compound having the [$AgCl_2^-$] anion is a new compound, compared to reported similar examples [37,38].

3.2. Antiproliferative effects

The antiproliferative effects of compounds **1**–**3** were tested against the human breast cancer cell line SKOV3. The compounds present extremely potent effects on cell viability, with IC_{50} values in the nM range. Specifically, compound **3** is the most potent of the series with an $IC_{50} = 0.20 \pm 0.05$ μM, while **1** and **2** have slightly higher values (ca. 0.4 μM for both compounds).

3.3. DNA binding studies

The primary intracellular target of antitumor drugs is DNA; so, drug–DNA interaction is of paramount importance and can lead to the primary mechanism of tumor inhibition for the treatment of cancer. Therefore, to obtain an insight into the binding propensity and binding mode, interaction of compounds **1**–**3** with calf thymus DNA (CT-DNA) was carried out by using absorption spectroscopy. Interaction of compounds with CT-DNA may result in an increase in absorbance (hyperchromism), or a decrease in absorbance (hypochromism). The

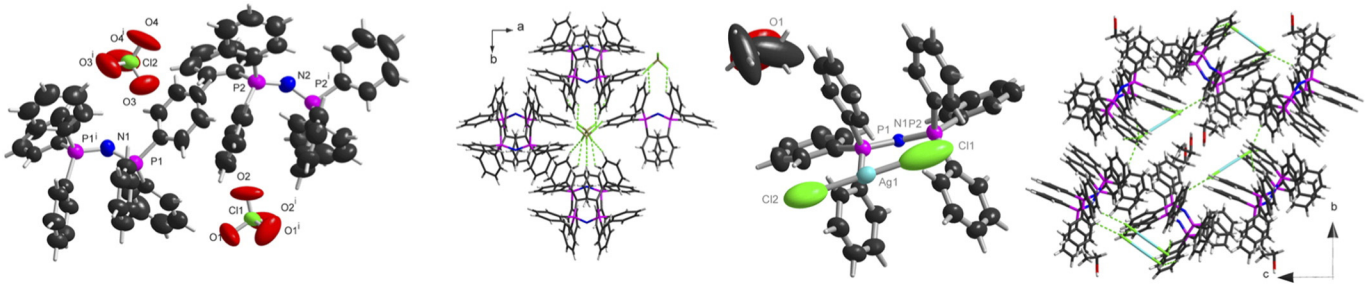

Fig. 2. Molecular depiction of the compounds **1**–**3**. From left to right thermal ellipsoidal of **1**, packing and hydrogen bonding of **2**, thermal ellipsoidal of **3** and packing with hydrogen bonding of **3**.

Please cite this article as: A. Folda, et al., Insights into the strong in-vitro anticancer effects for bis(triphenylphosphane)iminium compounds having perchlorate, tetrafluorid..., J. Inorg. Biochem. (2015), http://dx.doi.org/10.1016/j.jinorgbio.2015.08.030

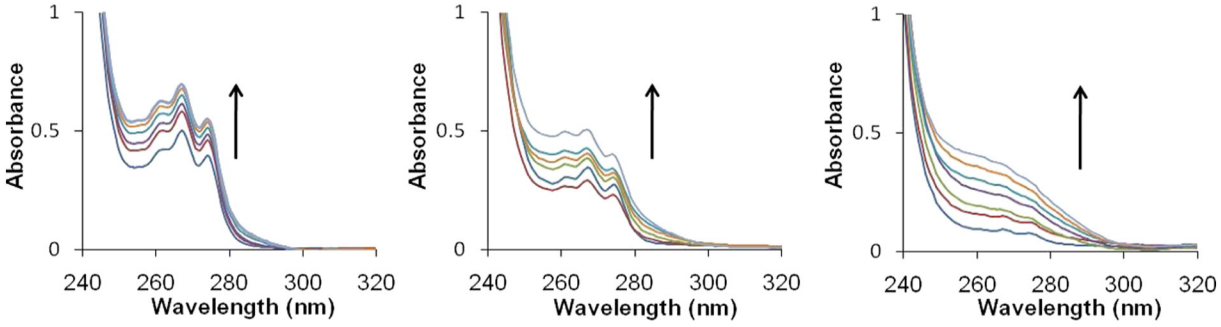

Fig. 3. Absorption spectra of compounds **1** (left), **2** (middle), and **3** (right) in Tris–HCl buffer (pH = 7.2) and in the presence of increasing amounts of CT-DNA. Arrows indicate the increase in the intensity upon increasing DNA concentration.

former suggests the rupture of the secondary structure of DNA, while the latter is the characteristic of intercalation [39] attributed to the interaction between the electronic states of the chromophore in the compound and those of the DNA bases [40].The binding interaction between the cationic compounds and CT-DNA leads to diffusion-limited ion-pair formation at higher concentration of the compound, such that the molecule is fitted to the contour of DNA double helix in an induced-fit fashion. Thus, the compounds preferably bind to the DNA helix via groove binding interactions. This groove binding results in structural reorganization of CT-DNA, which entails partial unwinding or damage of the double helix at the exterior phosphate backbone leading to the formation of a cavity to accommodate the molecule. Consequently, uptake occurs with partial melting of the double helix and generation of an appropriate binding pocket. The absorption spectra of compound **1**–**3** in the presence of CT-DNA are depicted in Fig. 3.

Upon the addition of increasing amounts ($0.067–0.33 \times 10^{-4}$ M) of CT-DNA to **1**–**3** of fixed concentration (0.067×10^{-4} M), concomitant increase in the absorption intensity was observed "hyperchromaticity". The observed hyperchromic effect suggests that the binding of the compounds to CT-DNA may be through an external contact (electrostatic and/or groove binding).

Furthermore, to evaluate quantitatively the binding strength of compounds **1**–**3** with CT-DNA, the intrinsic binding constant, K_b, was determined using Eq. (1) by monitoring the changes in absorbance of the π–π* bands with increasing concentration of CT-DNA,

$$[DNA]/|\varepsilon_a - \varepsilon_b| = [DNA]/|\varepsilon_b - \varepsilon_f| + 1/K_b/|\varepsilon_b - \varepsilon_f| \quad (1)$$

where [DNA] represents the concentration of DNA, ε_a, ε_f and ε_b are the apparent extinction coefficients A_{obs}/[complex], the extinction coefficient for the free compound and the extinction coefficient for the compound in the fully bound form, respectively. The intrinsic binding constants were found to be: **1** (2.96×10^4 M^{-1}), **2** (1.78×10^4 M^{-1}) and **3** (0.9×10^4 M^{-1}).

3.4. Ethidium bromide displacement assay

The competitive fluorescence displacement assay involves the addition of molecule to pretreated CT-DNA with ethidium bromide (EthBr), and the intensity of EthBr emission was measured. The addition of a second DNA-binding molecule can quench the emission intensity of DNA–EthBr adduct by either replacing EthBr and/or by accepting the excited-state electron of the EthBr through a photoelectron transfer mechanism [41].

The emission spectra of EthBr–DNA in the absence and presence of compounds **1**–**3** are depicted in Fig. 4. The addition of increasing amounts of compounds **1**–**3** to CT-DNA pretreated with ethidium bromide ([DNA] is 100 μM, [EthBr] = 10 μM) resulting in the quenching of emission intensity, that indicates displacement of the bound ethidium bromide from the CT-DNA by the complexes. This observation may suggest binding of complexes **1**–**3** to DNA via a groove binding mode and liberating few EthBr molecules from the EthBr–DNA system. The quenching of the fluorescence of ethidium bromide-bound DNA reveals the magnitude of DNA binding of compounds. Thus, we have evaluated quantitatively the quenching extents of complexes **1**–**3**, using the classical Stern–Volmer Eq. (2),

$$I_o/I = 1 + K_{SV}\, r \quad (2)$$

Where, I_o and I give the fluorescence intensities in the absence and the presence of complex, respectively. The concentration ratio of the complex to DNA is the value for "r". K_{SV} values are used to evaluate the quenching efficiency and are obtained as the slope of I_o/I vs. r. The K_{SV} values for compounds **1**–**3** were found to be 1.68, 1.22, and 0.95 M^{-1}, respectively. The DNA binding affinities of the compounds, therefore, follows the order **1** > **2** > **3**. Also, the apparent DNA binding constants (K_{app}) of the complexes **1**–**3** to CT DNA were calculated using the equation.

$$K_{EthBr}[EthBr] = K_{app}[complex]$$

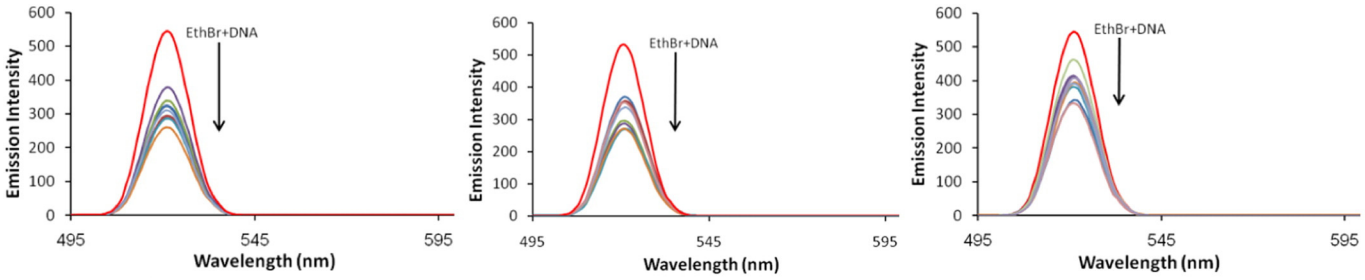

Fig. 4. Effect of addition of complexes **1** (left), **2** (middle) and **3** (right), on the emission intensity of DNA-EthBr in 5 mM Tris–HCl buffer at pH 7.1.

Please cite this article as: A. Folda, et al., Insights into the strong in-vitro anticancer effects for bis(triphenylphosphane)iminium compounds having perchlorate, tetrafluorid..., J. Inorg. Biochem. (2015), http://dx.doi.org/10.1016/j.jinorgbio.2015.08.030

where K_{EthBr} (4.94×10^5 M^{-1}) is the DNA binding constant of EthBr, [EthBr] is the concentration of EthBr (10 μM), and [complex] is the concentration of the complex which reduces the EthBr florescence intensity to 50%.The K_{app} values for **1–3** are 2.49×10^4, 2.21×10^4, and 1.53×10^4 M^{-1}, giving an order **1** > **2** > **3**, in conformity from absorption spectral studies.

3.5. Analysis of mitochondrial functions

Since the PPN^+ moiety could behave as a Delocalized Lypophilic Cation (DLC) type of compound, we decided to investigate the effects of **1–3** on the mitochondria. It is worth mentioning that DLCs have been explored as an approach to cancer chemotherapy that exploits their selective accumulation in mitochondria of cancer cells, as a consequence of the elevated transmembrane mitochondrial potential $\Delta\psi_m$[20]. In fact, DLCs can pass easily through the lipid bilayer and their positive charge then directs them to the mitochondria where they accumulate at significantly higher concentrations than in the cytoplasm, owing to the large $\Delta\psi_m$ generated by the respiratory chain [42]. Thus, the effects on isolated mitochondria of compounds **1–3** were evaluated by estimation of the principal parameters of mitochondrial functions. As shown in Fig. 5, mitochondrial swelling (A) and membrane potential (B) have been examined.

Compounds **1** and **2** are able to induce swelling at a relatively high concentration (40 μM), while compound **3** causes a marked swelling at lower concentrations (5–10 μM). With the same compound, swelling occurs also at very low concentrations (1, 2.5 μM) and is preceded by a lag of about 4 to 8 min. All three compounds, at 10 μM concentration, determine a large and rapid decrease of the membrane potential that is particularly extensive for compound **3**. This decrease might be referred to the nature of delocalized lipophilic cations.

Finally, mitochondrial respiration in the presence of compounds **1–3** was also measured. As reported in Fig. 6, addition of compound **1** and **2,** at 10 μM concentration, induces an increase of succinate-dependent respiration that is not further stimulated by the subsequent addition of the classical uncoupling agent CCCP (Carbonyl cyanide *m*-chlorophenyl

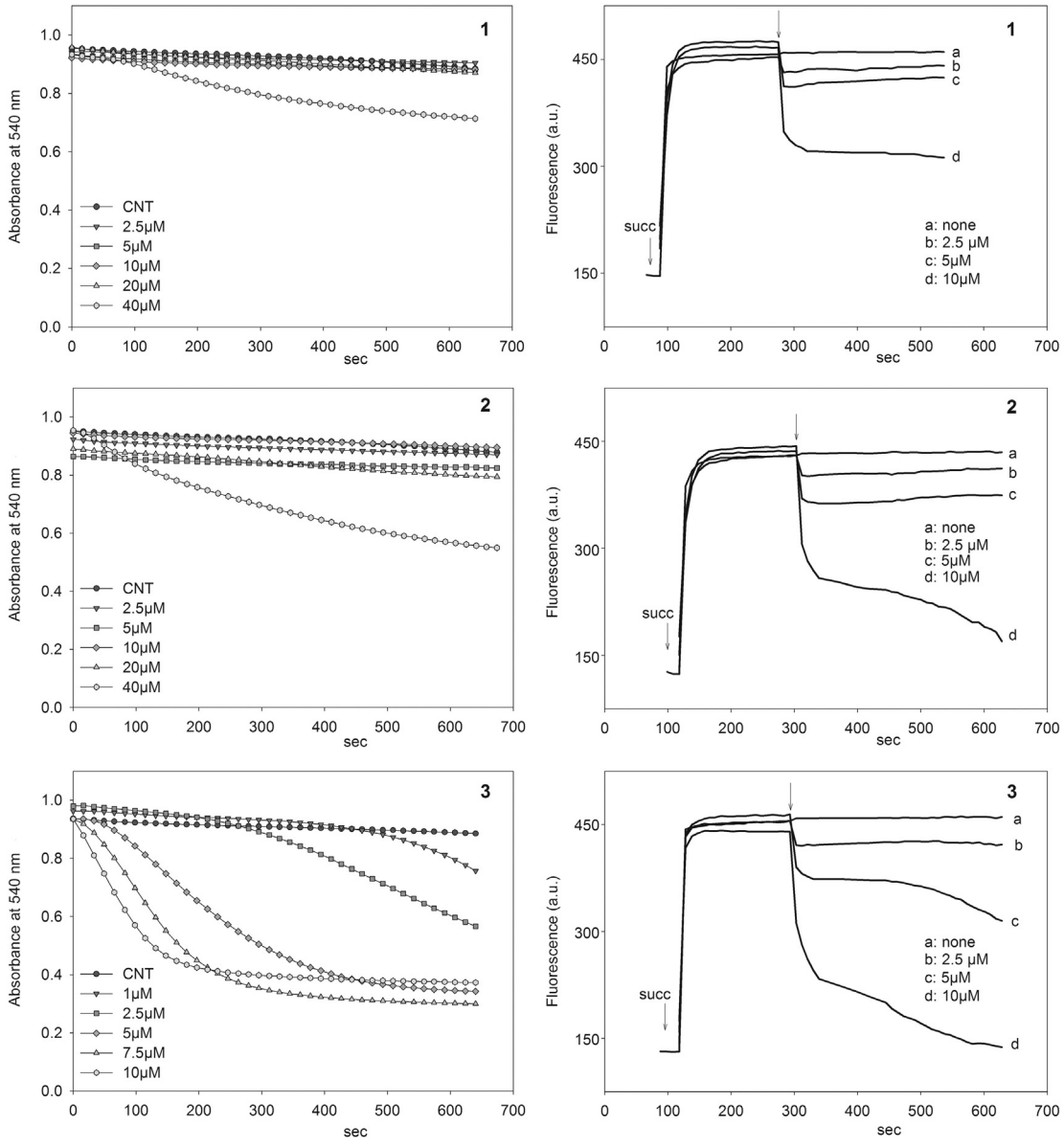

Fig. 5. Induction of mitochondrial swelling by increasing concentrations of **1–3** (left) and the effect of compounds **1–3** on the mitochondrial membrane potential (right). Rat liver mitochondria (0.25 mg/mL) were incubated at 25 °C in 213 mM mannitol, 71 mM sucrose, 5 mM Hepes/Tris buffer (pH 7.4), 5 mM succinate, and 3 mg/mL rotenone. Mitochondrial swelling was followed spectrophotometrically at 540 nm. Compounds **1–3** were used at the indicated concentrations. The mitochondrial membrane potential was determined with rhodamine 123, as described in the experimental section. Compounds **1–3** were added where arrows are indicated.

Please cite this article as: A. Folda, et al., Insights into the strong in-vitro anticancer effects for bis(triphenylphosphane)iminium compounds having perchlorate, tetrafluorid..., J. Inorg. Biochem. (2015), http://dx.doi.org/10.1016/j.jinorgbio.2015.08.030

hydrazone), but instead an inhibitory effect takes place and increases with time.

Compound **3** markedly inhibits respiration, and is also completely insensitive to the uncoupling agent CCCP. The inset of Fig. 6 shows a control experiment reporting the stimulation of respiration by ADP and the subsequent oxygen uptake by the uncoupler CCCP. It should be noted that the increase of respiration occurring in the presence of compounds **1** and **2**, at least at the beginning, is independent of the swelling of the mitochondria, as the latter is a slower event with respect to respiration. However, by comparing the rates of respiration occurring after CCCP addition in the control experiment with those obtained in the presence of compounds **1** and **2**, it is clearly evident that, after an initial stimulation, compounds **1** and **2** progressively inhibit mitochondrial respiration.

The mitochondrial membrane potential was also analyzed in cancer cells. A2780 cells (6×10^5) were incubated with 5 μM of compound **1–3** for 18 h and then subjected to flow cytometry analysis using 25 nM TMRM (tetramethylrhodamine). As reported in Fig. 7 all three compounds lead to a strong decrease in the number of fluorescent cells and, in particular, compound **3** causes a dramatic loss of mitochondrial membrane potential. Table 3 summarizes the percentage of cells with high and low fluorescence, reported as an average ±SD of five experiments.

3.6. Mitochondrial thioredoxin reductase inhibition

In mitochondria, thioredoxin reductase (TrxR2) is present in the matrix fraction. As apparent in Fig. 8 compounds **1** and **2** are able to inhibit TrxR2 at micromolar level (as results from their IC_{50}) and this inhibition is possibly related to their cationic structure. Compound **3** determines a strong inhibition on TrxR2 at nanomolar level ($IC_{50} = 2.75$ nM). The latter effect might partly depend on the presence of the $[AgCl_2^-]$ moiety, as silver compounds are known as effective inhibitors of thioredoxin reductase [43,44]. PPN^+ compounds after entering mitochondria by exploiting the membrane potential can act on different intramitochondrial functional targets. A marked energetic impairment takes place, as shown by the very effective decrease of the membrane potential exerted by the PPN^+ compounds on isolated mitochondria and cultured cells (see Figs. 5 and 7). Among the potential targets subjected to the action of PPN^+ we have examined mitochondrial thioredoxin reductase. This enzyme is endowed with a C-terminal motif characterized by the sequence -Cys-SeCys-Gly, which is also the site of inhibition of several agents, especially gold and platinum complexes and electrophilic compounds many of which are also anticancer agents [21].

However, also cations such as Ca^{2+} and La^{3+} were shown to act as inhibitors of TrxR although possibly at a site different from the C-terminal. Their effect was attributed to an interaction with anionic groups of the enzyme as also apparent from the preventive effect exerted by the ion chelator H_4edta [45,46]. In the present study we show that also PPN^+ compounds can act as inhibitors of thioredoxin reductase showing values for IC_{50} in the range of 5–10 μM. Although these figures are higher in comparison to those obtained with other inhibitors, such as gold compounds that act at nanomolar levels [47], it should be noted that DLC concentrate hundreds of times in the mitochondrial matrix [16]. Therefore, inside the mitochondrion the PPN^+ compounds under study should easily reach concentrations able to completely prevent the activity of thioredoxin reductase. The effect of Ca^{2+} and La^{3+} is electrostatic in nature and PPN^+ compounds might act in a similar way by binding to anionic sites located inside tumor cell mitochondria.

Considering the differential inhibitory effect on thioredoxin reductase exhibited by the PPN^+ compounds containing different anions (Fig. 8), it is apparent that these play a relevant role in eliciting the inhibitory properties on thioredoxin reductase. It is interesting to note that the anions ClO_4^- and BF_4^- alone are completely ineffective on thioredoxin reductase at concentrations until 100 μM (data not shown).

Furthermore, we observed that PPNCl still inhibits thioredoxin reductase, although at concentrations higher ($IC_{50} > 40$ μM) than those observed with the other compounds (data not shown). The effects of compounds **1–3** were also tested on cytosolic thioredoxin reductase (TrxR1) and on glutathione reductase (GR) (see Table S1 of the Electronic Supporting Information). As apparent, compounds **1–3** inhibit TrxR1 at concentrations comparable to those observed for TrxR2. In

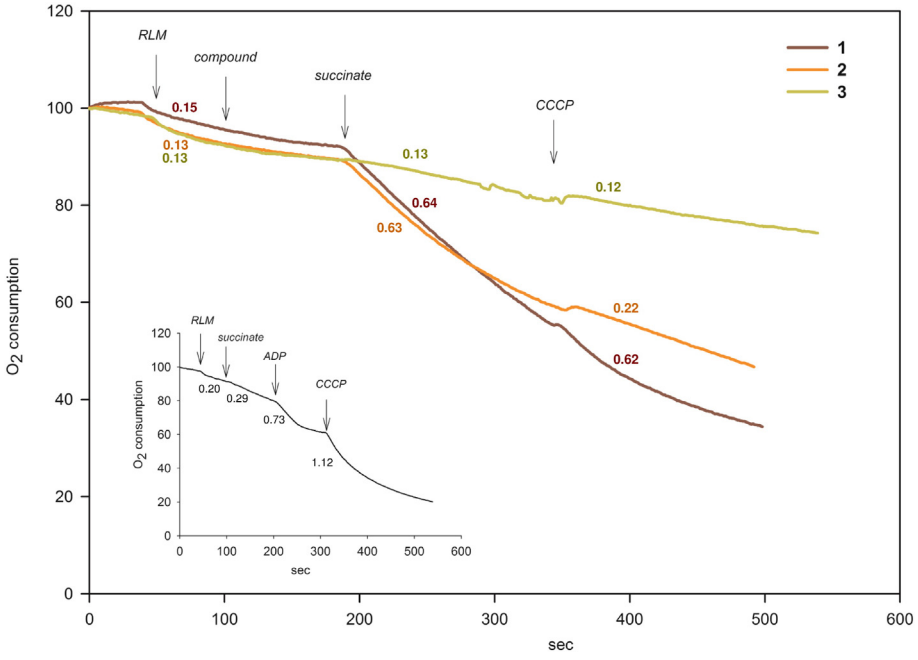

Fig. 6. Effects of compounds **1–3** on mitochondrial dioxygen uptake. Rat liver mitochondria were incubated with 10 μM compounds **1–3** in the presence, where indicated, of 7.5 mM succinate and 0.1 μM CCCP. Numbers by each line indicate dioxygen consumption rate (nmoles O_2 $sec^{-1}mg^{-1}$ protein). *Inset*: control experiment showing the stimulation of respiration by 0.2 mM ADP.

Please cite this article as: A. Folda, et al., Insights into the strong in-vitro anticancer effects for bis(triphenylphosphane)iminium compounds having perchlorate, tetrafluorid..., J. Inorg. Biochem. (2015), http://dx.doi.org/10.1016/j.jinorgbio.2015.08.030

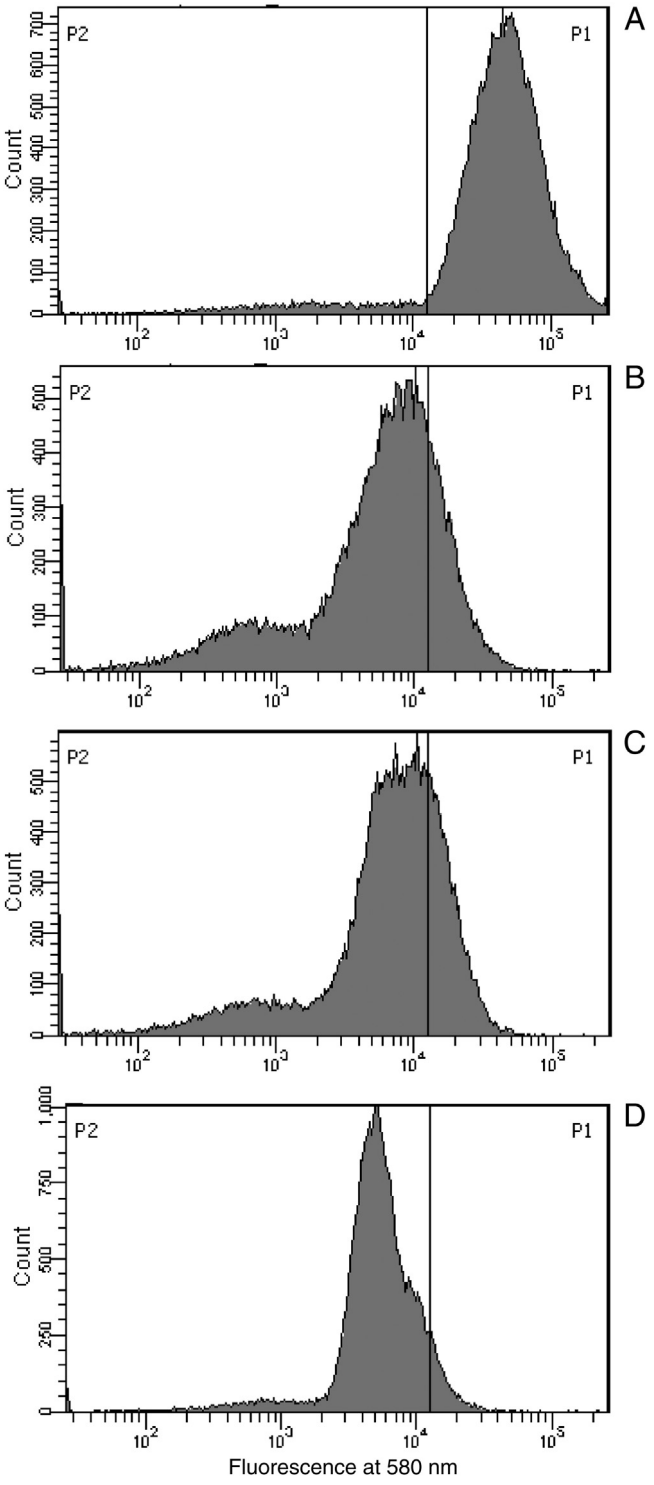

Fig. 7. Decrease of membrane potential in A2780 cells in the presence of compounds **1–3**. A2780 cells, treated for 18 h with 5 μM of compounds **1-3**, were incubated with 25 nM TMRM for 20 min and then analyzed by flow cytometry. A, control; B, compound **1**, C, compound **2**; D, compound **3.**

Table 3
Percentage of cells with high and low mitochondrial membrane potential (MMP) after treatment with compounds **1–3**.

Sample	High MMP	Low MMP
Control	91.2 ± 2.6	08.1 ± 1.2
1	40.3 ± 4.2	59.2 ± 5.4
2	36.6 ± 3.4	61.4 ± 3.2
3	13.7 ± 1.3	84.1 ± 2.1

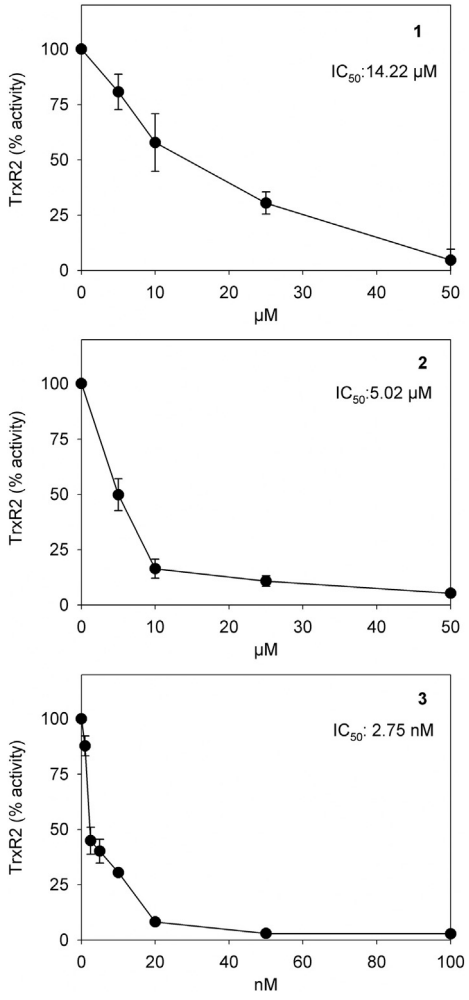

Fig. 8. Mitochondrial thioredoxin reductase inhibition by compounds **1, 2** and **3.** Aliquots of highly purified TrxR2 were incubated in the presence of increasing concentrations of compounds **1–3**, and the reaction was followed at 412 nm, as indicated under experimental methods.

contrast, compounds **1** and **2** are ineffective on GR, while compound **3** markedly inhibits this enzyme.

TrxR is considered a major target of the inhibitory effect of a large number of anticancer agents and its inhibition leads to cell death [21]. However, it should also be considered that PPN^+ compounds, once inside the mitochondrion, can exert their inhibitory action on other targets in addition to TrxR. It is noted that other DLCs, such as tetraphenylphosphanium or rhodamine-123 tested in the same experimental conditions are ineffective on TrxR activity. However, brilliant green, which is a cationic triphenylmethane, was shown to exert a disruptive effect on the mitochondrial thioredoxin system [48].

4. Concluding remarks

The results described and discussed above strongly suggest that salts of the bis(triphenylphosphane)iminium cation do show significant anticancer activity, DNA binding and also inhibition of the enzyme thioredoxin reductase, as well as causing mitochondrial damage. The role of the used counter anions, i.e. perchlorate (**1**), tetrafluoridoborate (**2**) and dichloridoargentate(I) (**3**), was relevant for the specific properties of each compound, as they differentiate their reactivity in a biological context. Compound **1** appeared to be less effective than compound **2**, however, the strongest effects were found for compound **3**. These differences observed for thioredoxin reductase inhibition and mitochondrial functions alteration, were found also reflected in other

Please cite this article as: A. Folda, et al., Insights into the strong in-vitro anticancer effects for bis(triphenylphosphane)iminium compounds having perchlorate, tetrafluorid..., J. Inorg. Biochem. (2015), http://dx.doi.org/10.1016/j.jinorgbio.2015.08.030

measurements, like DNA binding. The effect of compound **3** toward thioredoxin reductases and glutathione reductase is significantly larger than that of compounds **1** and **2**, and is most likely due to the role played by the Ag^+ ions known to inhibit TrxR [43,44]. In fact the selenocysteine residue present in the C-terminal motif of TrxR is sensitive to several inhibitors, including some metal ions [21].

The present results have also made clear that the PPN^+ cation can determine an energetic impairment, resulting in a strong decrease of the mitochondrial membrane potential, which, associated with thioredoxin reductase inhibition, may play a relevant role in the possible toxic effects of these compounds in cancer cells, together with other mechanisms (e.g. DNA damage). Further studies are necessary to demonstrate the selectivity of such biological activity in cancer cells with respect to non-cancerous ones, and to develop PPN^+ compounds especially targeted to mitochondria of diseased tissues therefore addressing cancer cell to death.

Acknowledgments

The authors are indebted to several sources of funding for this project. The authors acknowledge PRIN20107Z8XBW granted by Ministero dell'Istruzione, Università e Ricerca (MIUR) Italy, CPDA130272 granted by University of Padova (Italy) and COST ActionsCM1105. Also thanks are due to the Distinguished Scientific Fellows Programme of King Saud University, for financial support.

Appendix A. Supplementary data

Electronic supplementary information (ESI) available: Crystallographic, structural data and figures of compound **1, 2** and **3**. See CCDC reference numbers 1,403,185 (**1**), 1,403,186 (**2**) and 1,403,187 (**3**). These data can be obtained free of charge via http://www.ccdc.cam.ac.uk/conts/retrieving.html, or from the Cambridge Crystallographic Data Centre, 12 Union Road, Cambridge CB2 1EZ, UK; fax: (+44) 1223–336–033; or e-mail: deposit@ccdc.cam.ac.uk. Supplementary data to this article can be found online at http://dx.doi.org/10.1016/j.jinorgbio.2015.08.030.

References

[1] P. Paul, Z.W. Xie, R. Bau, P.D.W. Boyd, C.A. Reed, J. Am. Chem. Soc. 116 (1994) 4145–4146.
[2] H. Moriyama, H. Kobayashi, A. Kobayashi, T. Watanabe, J. Am. Chem. Soc. 115 (1993) 1185–1187.
[3] J.K. Evju, K.R. Mann, Chem. Mater. 11 (1999) 1425–1433.
[4] R.D. Wilson, R. Bau, J. Am. Chem. Soc. 96 (1974) 7601–7602.
[5] CSD, CSD, Cambridge Crystallographic Data Center, 2015.
[6] R.E. Stevens, T.J. Yanta, W.L. Gladfelter, J. Am. Chem. Soc. 103 (1981) 4981–4982.
[7] G. Werner, I. Kolowos, J. Senkyr, Talanta 36 (1989) 966–968.
[8] C. Glidewell, H.D. Holden, J. Organomet. Chem. 226 (1982) 171–181.
[9] F. Seel, R. Kuhn, G. Simon, Z. Naturforsh. B 39 (1984) 1622–1623.
[10] F. Seel, R. Kuhn, G. Simon, M. Wagner, B. Krebs, M. Dartmann, Z. Naturforsh. B 40 (1985) 1607–1617.
[11] M.A. Beckett, P.N. Horton, M.B. Hursthouse, J.L. Timmis, Acta Crystallogr. Sect. E: Struct. Rep. Online 66 (2010) O319–U2063.
[12] K.F. Tebbe, N. Krauss, Acta Crystallogr. Sect. C: Cryst. Struct. Commun. 46 (1990) 878–880.
[13] C. Knapp, R. Uzun, Acta Crystallogr. Sect. E: Struct. Rep. Online 66 (2010) O3185–U3783.
[14] R.Y. Liau, H. Ehlich, A. Schier, H. Schmidbaur, Z. Naturforsh. B 57 (2002) 1085–1089.
[15] J.T. Madak, N. Neamati, Curr. Top. Med. Chem. 15 (2015) 745–766.
[16] M.P. Murphy, Biochim. Biophys. Acta Bioenerg. 1777 (2008) 1028–1031.
[17] S.J. Berners-Price, A. Filipovska, Aust. J. Chem. 61 (2008) 661–668.
[18] S. Rodriguez-Enriquez, A. Marin-Hernandez, J.C. Gallardo-Perez, L. Carreno-Fuentes, R. Moreno-Sanchez, Mol. Nutr. Food Res. 53 (2009) 29–48.
[19] M. Kurtoglu, T.J. Lampidis, Mol. Nutr. Food Res. 53 (2009) 68–75.
[20] J.S. Modica-Napolitano, J.R. Aprille, Adv. Drug Deliv. Rev. 49 (2001) 63–70.
[21] A. Bindoli, M.P. Rigobello, G. Scutari, C. Gabbiani, A. Casini, L. Messori, Coord. Chem. Rev. 253 (2009) 1692–1707.
[22] Rigaku, Crystal Clear. Crystal Structure Analysis Package, Rigaku, 9009 New Trails Dr., The Woodlands TX 77381, 2007.
[23] G.M. Sheldrick, Acta Crystallogr. A 64 (2008) 112–122.
[24] K. Brandenburg, Diamond, 3.1–6, DIAMOND, ver 3.1d, Crystal Impact GbR, Bonn, Germany, 2006.
[25] J.R. Lakowicz, G. Weber, Biochemistry 12 (1973) 4161–4170.
[26] M.E. Reichmann, S.A. Rice, C.A. Thomas, P. Doty, J. Am. Chem. Soc. 76 (1954) 3047–3053.
[27] A. Wolfe, G.H. Shimer, T. Meehan, Biochemistry 26 (1987) 6392–6396.
[28] R.A. Khan, F. Arjmand, S. Tabassum, M. Monari, F. Marchetti, C. Pettinari, J. Organomet. Chem. 771 (2014) 47–58.
[29] R.A. Khan, A. Asim, R. Kakkar, D. Gupta, V. Bagchi, F. Arjmand, S. Tabassum, Organometallics 32 (2013) 2546–2551.
[30] R.A. Khan, S. Yadav, Z. Hussain, F. Arjmand, S. Tabassum, Dalton Trans. 43 (2014) 2534–2548.
[31] D.K. Myers, E.C. Slater, Biochem. J. 67 (1957) 558–572.
[32] A.G. Gornall, C.J. Bardawill, M.M. David, J. Biol. Chem. 177 (1949) 751–766.
[33] F. Cazzaro, M.P. Rigobello, A. Bindoli, Comput. Methods Prog. Biomed. 51 (1996) 141–151.
[34] M. Luthman, A. Holmgren, Biochemistry 21 (1982) 6628–6633.
[35] M.P. Rigobello, A. Bindoli, in: E. Cadenas, L. Packer (Eds.), Methods in Enzymology, Thiol Redox Transitions in Cell Signaling, Pt B: Cellular Localization and Signaling, Vol 474, Elsevier Academic Press Inc., San Diego 2010, pp. 109–122.
[36] O.H. Lowry, N.J. Rosebrough, A.L. Farr, R.J. Randall, J. Biol. Chem. 193 (1951) 265–275.
[37] S. Aboulkacem, W. Tyrra, I. Pantenburg, J. Chem. Crystallogr. 36 (2006) 141–145.
[38] G.A. Bowmaker, M.I. Bruce, B.W. Skelton, N. Somers, A.H. White, Z. Anorg. Allg. Chem. 633 (2007) 1024–1030.
[39] T. Afrati, A.A. Pantazaki, C. Dendrinou-Samara, C. Raptopoulou, A. Terzis, D.P. Kessissoglou, Dalton Trans. 39 (2010) 765–775.
[40] B.D. Wang, Z.Y. Yang, P. Crewdson, D.Q. Wang, J. Inorg. Biochem. 101 (2007) 1492–1504.
[41] B. Selvakumar, V. Rajendiran, P.U. Maheswari, H. Stoeckli-Evans, M. Palaniandavar, J. Inorg. Biochem. 100 (2006) 316–330.
[42] M.F. Ross, G.F. Kelso, F.H. Blaikie, A.M. James, H.M. Cocheme, A. Filipovska, T. Da Ros, T.R. Hurd, R.A.J. Smith, M.P. Murphy, Biochem. Mosc. 70 (2005) 222–230.
[43] A. Citta, E. Schuh, F. Mohr, A. Folda, M.L. Massimino, A. Bindoli, A. Casini, M.P. Rigobello, Metallomics 5 (2013) 1006–1015.
[44] M. Srivastava, S. Singh, W.T. Self, Environ. Health Perspect. 120 (2012) 56–61.
[45] A. Citta, A. Folda, G. Scutari, L. Cesaro, A. Bindoli, M.P. Rigobello, J. Inorg. Biochem. 117 (2012) 18–24.
[46] M.P. Rigobello, F. Vianello, A. Folda, C. Roman, G. Scutari, A. Bindoli, Biochem. Biophys. Res. Commun. 343 (2006) 873–878.
[47] S. Gromer, L.D. Arscott, C.H. Williams, R.H. Schirmer, K. Becker, J. Biol. Chem. 273 (1998) 20096–20101.
[48] X. Zhang, Y.J. Zheng, L.E. Fried, Y.T. Du, S.J. Montano, A. Sohn, B. Lefkove, L. Holmgren, J.L. Arbiser, A. Holmgren, J. Lu, Free Radic. Biol. Med. 50 (2011) 811–820.